

Wind models for O-type stars

T. L. Hoffmann & A. W. A. Pauldrach, University of Munich

email: hoffmann@usm.uni-muenchen.de, uh10107@usm.uni-muenchen.de

http://www.usm.uni-muenchen.de/people/adi/adi.html

Abstract

Spectral analysis of hot stars requires adequate model atmospheres which take into account the effects of NLTE and radiation-driven winds properly. Here we present significant improvements of our approach in constructing detailed atmospheric models and synthetic spectra for O-type stars. The most important ingredients of our models with regard to a realistic description of stationary winds are:

- A sophisticated and consistent description of line blocking and blanketing that renders the line blocking influence on the ionizing fluxes in identical quality as the synthetic high-resolution spectra, as well as properly accounting for the line blanketing effect in the energy balance.
- A consistent determination of the radiative line acceleration and solution of the hydrodynamics.
- A considerably improved and enhanced atomic data archive providing the basis for a detailed multilevel NLTE treatment of the metal ions (from C to Zn) and an adequate representation of line blocking and the radiative line acceleration.
- Inclusion of EUV and X-ray radiation produced by cooling zones originating from shock-heated matter.

This new tool not only provides a method for O-star diagnostics (whereby physical constraints on the properties of stellar winds, stellar parameters, and abundances can be obtained via a comparison of observed and synthetic spectra), but also allows the astrophysically important information about the ionizing fluxes of these stars to be determined.

Description of Method

The basis for our approach in constructing detailed atmospheric models for hot luminous stars is the concept of *homogeneous, stationary, and spherically symmetric radiation-driven winds*, where the expansion of the atmosphere is due to scattering and absorption of radiation by Doppler-shifted metal lines.

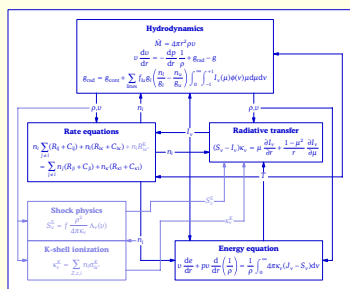


FIGURE 1. — Overview of the physics of radiation-driven winds.

The required physics (see Figure 1) are solved in a series of nested iteration cycles as illustrated in Figure 2. (A detailed description of the method is given in Pauldrach et al. 2001.) As a result of the solution of this system we obtain not only the synthetic spectra and ionizing fluxes (which can be used in order to determine stellar parameters and abundances via comparison with observed spectra), but also the hydrodynamical structure of the wind (thus, constraints on the mass loss rate and velocity field can be obtained).

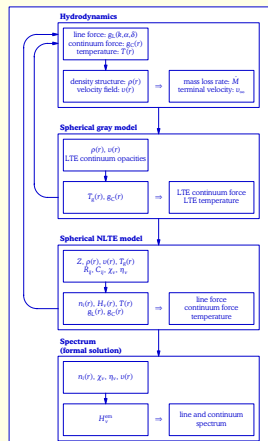


FIGURE 2. — Schematic sketch of a model run.

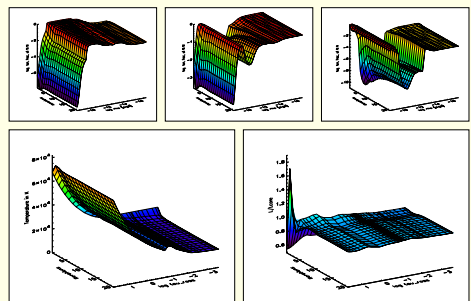


FIGURE 3. — Temperature (left), flux conservation (right), and ionization fractions of nitrogen (top) vs. depth and iteration block number for a 29000 K supergiant model.

For comparison with observations, a high-resolution synthetic spectrum is calculated from the converged model using the same radiative transfer routine as in the NLTE program. An example is shown in Figure 4.

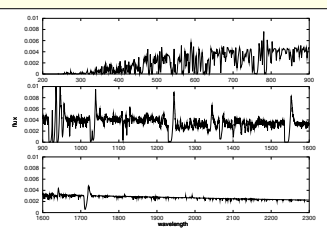


FIGURE 4. — Synthetic high-resolution spectrum computed for a 45000 K supergiant model.

Comparison with observations

From the large sample of Galactic stars for which mass loss rates and stellar parameters have been determined by Puls et al. (1996) we have selected a representative subsample to compare against our model calculations. The parameters are listed in Table 1.

star	T_{eff}	$\log g$	R	\dot{M}	v_∞	$\log g$	R	\dot{M}	v_∞
HD 93250	50500	4.00	18	4.9	3250	10	3200		
HD 93129A	50500	3.95	20	22	3200	14	3200		
HD 68811 (ζ Pup)	42000	3.60	19	5.9	2250	7.5	2000		
HD 217086	40000	3.75	10	≤ 0.2	2550	0.55	2600		
HD 30614 (α Cam)	30000	3.00	29	5.2	1550	2.6	1500		

TABLE 1. — Parameters of the sample stars. Radii are in solar radii, mass loss rates in $10^{-6} M_\odot/\text{yr}$, terminal velocities in km/s.

The results are very encouraging: not only do our models reproduce the observed terminal velocities to within 10% and the mass loss rates to within about a factor of 2 (see Figure 5), but at the same time also represent the observed UV spectra quite well (Figure 6). (Note, however, that the analysis by Puls et al. did not consider line blanketing; the sample has recently been reanalyzed taking this effect into account.)

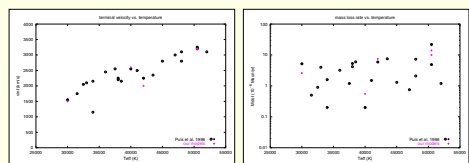


FIGURE 5. — Terminal velocities (left panel) and mass loss rates (right panel) of our sample stars compared with the values obtained by Puls et al. (1996).

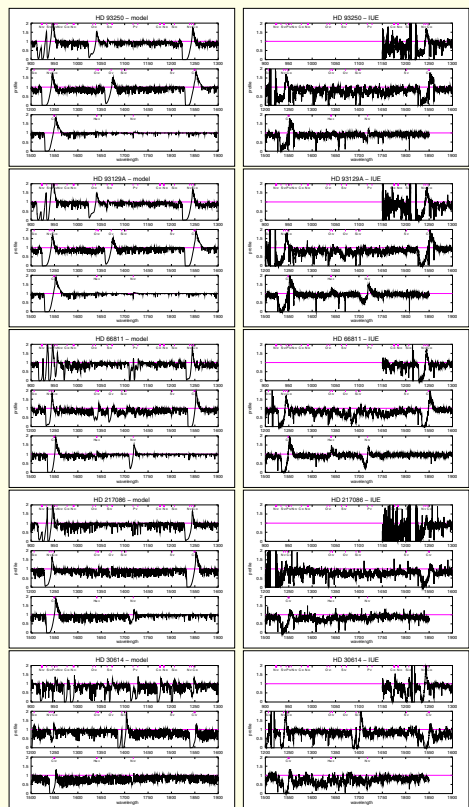


FIGURE 6. — Comparison of synthetic model spectra with observed spectra of stars with similar stellar parameters.

Discrepancies to the observed UV spectra can be eliminated by fine-tuning the stellar parameters (and the abundances), as explained in the next section. Figure 7 shows the UV spectrum of the α Cam model additionally incorporating shock radiation, as well as the corresponding EUV flux and a comparison with the ROSAT observations.

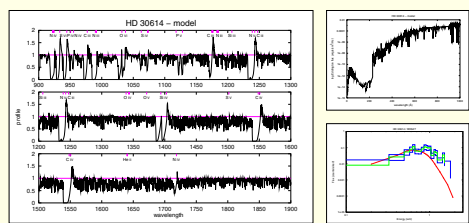


FIGURE 7. — UV spectrum of a model for α Cam including shocks (left), its EUV flux (right top), and a comparison with the observed ROSAT flux (right bottom).

Determining stellar parameters

Computing the wind dynamics consistently permits not only the determination of wind parameters from given stellar parameters, but, conversely, makes it possible to obtain the stellar parameters from the observed UV spectrum alone. The basic procedure for determining the stellar parameters from the observed UV spectrum is outlined in Figure 8.

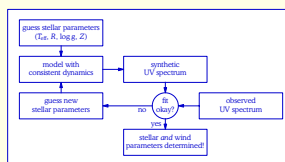


FIGURE 8. — Determining stellar parameters through UV spectral analysis.

This idea is not new (see, for example, Kudritzki et al. 1992); however, only now are the models beginning to reach a degree of sophistication that makes such a procedure useful in practice. An application of the method to O-type central stars of planetary nebulae is given by Pauldrach et al. 2004.

To briefly illustrate the effect of a change in radius and gravity on the spectra and wind parameters, we have calculated a grid of models with consistent wind dynamics, using radii R from 15 to 25 R_\odot and surface gravities $\log g$ from 3.4 to 4.0 (at a temperature of $T_{\text{eff}} = 40000$ K). The resulting mass loss rates and terminal velocities are plotted in Figure 9; the corresponding UV spectra are shown in Figure 10.

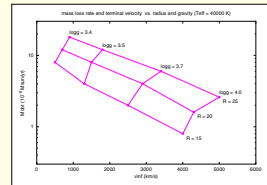


FIGURE 9. — Consistent terminal velocities and mass loss rates for a grid of 40000 K models with radii from 15 to 25 R_\odot and $\log g$ from 3.4 to 4.0.

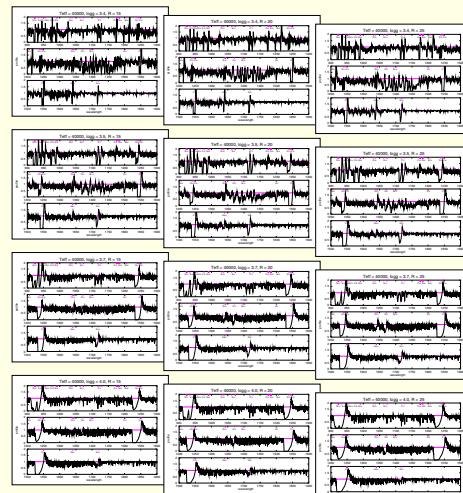


FIGURE 10. — Synthetic UV spectra of the above grid models.

For example, lowering the temperature of the model for α Cam to 29000 K and increasing the radius to 35 R_\odot to obtain a higher mass loss rate leads to a much better agreement with the observed spectrum, as shown in Figure 11 (shock radiation is also included in this model).

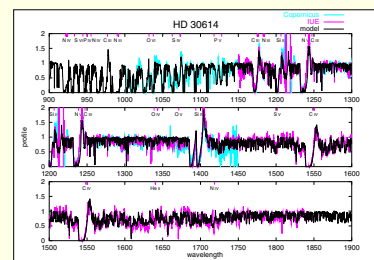


FIGURE 11. — Synthetic spectrum of a model for α Cam with $T_{\text{eff}} = 29000$ K and $R = 35 R_\odot$ compared with the observed Copernicus and IUE spectra.

References

- Kudritzki R.-P., Hummer D. G., Pauldrach A. W. A., et al., *A&A* 257, 655 (1992)
 Pauldrach A. W. A., Hoffmann T. L., Mészáros R. H., *A&A* 419, 1111 (2004)
 Pauldrach A. W. A., Hoffmann T. L., Lennon M., *A&A* 375, 161 (2001)
 Puls J., Kudritzki R.-P., Herrero A., et al., *A&A* 307, 171 (1996)